

Phase diagram of poly(methyl-*p*-tolyl-siloxane): A temperature- and pressure-dependent dielectric spectroscopy investigation

K. Mpoukouvalas and G. Floudas*

*Department of Physics, University of Ioannina, P.O. Box 1186, 451 10 Ioannina, Greece**and Foundation for Research and Technology–Hellas (FORTH), Biomedical Research Institute (BRI), Ioannina, Greece*

(Received 5 April 2003; published 11 September 2003)

The dynamics of poly(methyl-*p*-tolyl-siloxane) (PMpTS) have been studied as a function of temperature (in the range from 143 to 413 K), pressure (0.1–300 MPa), frequency (10^{-2} – 10^6 Hz), and molecular weight. Independent pressure-volume-temperature (PVT) measurements (for temperatures in the range from 293 to 393 K and for pressures in the range from 10 to 200 MPa) allowed calculation of the relevant thermodynamic parameters. Two dielectrically active channels of relaxation were found, one in the glassy state reflecting a localized motion of the substituted phenyl ring and one at higher temperatures reflecting the usual segmental (α) relaxation. In PMpTS, there are two dominant control variables; both density and temperature have a strong influence on the segmental dynamics. The PVT results allowed us to follow distinct thermodynamic (T, P) paths resulting in states bearing the same density. These isodensity states are characterized by an apparent activation energy (Q_V) that is not very different from the corresponding activation energy under isobaric conditions ($Q_V/Q_P \sim 0.55$) reflecting the importance of thermal effects. At temperatures above the glass temperature (T_g), strong orientation correlations exist above some critical pressure that depends on temperature. This state extends from T_g up to $1.08 T_g$ and separates a normal liquid at higher temperatures from an oriented liquid at lower temperatures. Using the “phase diagram” we discuss separately the influence of the temperature and density on the PMpTS dynamics.

DOI: 10.1103/PhysRevE.68.031801

PACS number(s): 36.20.-r, 64.70.Md, 61.41.+e, 77.84.Nh

I. INTRODUCTION

The effect of pressure on polymer dynamics has been rejuvenated as a result of novel polymer synthesis but more importantly due to the availability of more versatile experimental tools [1]. Earlier studies [2,3] of the application of pressure have shown that this is the right variable if a separation of the segmental (α) from the more local β process is needed. We have recently examined the effect of pressure on (i) the local and chain polymer dynamics of type-A polymers (polymers bearing a dipole moment along the backbone) [4–6], (ii) the process of polymer crystallization [7] and the associated kinetics by performing pressure-jump experiments [8], (iii) the miscibility of block copolymers and polymer blends [9], (iv) the dynamics of hairy-rod polymers with potential use in lithium-ion batteries [10], and (v) the complex dynamics in polymer liquid crystals with emphasis on the construction of the relevant phase diagrams [11]. Several other studies of the segmental dynamics in amorphous polymers [12–14] including polyelectrolytes [15] and glass-forming liquids [16–18] as a function of pressure have recently appeared, aiming at establishing a connection between the chemical structure and the characteristics of their local relaxation.

Recent investigations [19] in glass-forming liquids explored the possibility that the dynamic arrest at the glass temperature (T_g), known as “glass transition,” is due to a single control variable. The question of whether glass formation is associated primarily with the decrease of the available volume (and thus of the available free volume) or with

purely thermally activated processes (i.e., with the existence of energy barriers large compared to kT) is of central interest in understanding glass formation. Investigations in some glass-forming liquids and polymers suggested that glass formation is associated with insufficient thermal energy caused by lowering temperature as opposed to a decrease in the available volume, suggesting temperature (T) as the main control parameter. A change in temperature, however, has two opposite effects; change in thermal energy and in density. Pressure offers the possibility to disentangle the two effects, since a change in pressure together with a change in temperature allows controlled variations of both temperature and density along distinct thermodynamic paths.

In the present investigation, we test the importance of the two parameters (density and temperature) in the process of glass formation by employing poly(methyl-*p*-tolyl-siloxane) (PMpTS), a polymer studied earlier by light scattering [20] and dielectric spectroscopy [21] techniques. The light-scattering investigation revealed the existence of long-range density fluctuations (i.e., clusters) characterized by an excess angular-dependent isotropic scattered intensity and an additional slow decay in the photon correlation function. Herein, we use temperature- and pressure-dependent dielectric spectroscopy in combination with pressure-volume-temperature (PVT) measurements on two PMpTS samples with different molecular weights. We find that, in PMpTS, both density and temperature have a strong influence on the segmental dynamics. Furthermore, the PVT results allow a comparison of the different activation energies involved as well as construction of the relevant “phase diagram.” Using this “phase diagram” we discuss separately the influence of the temperature and density on the PMpTS dynamics.

*Corresponding author. Email address: gfloudas@cc.uoi.gr

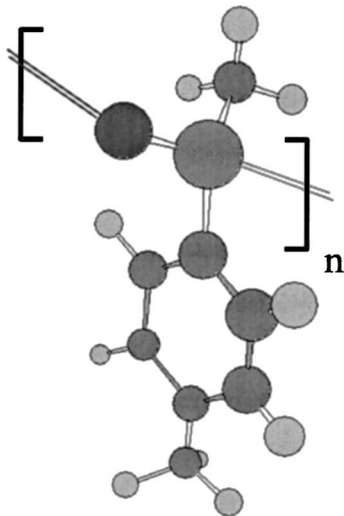


FIG. 1. Structure of the repeat unit in PMpTS.

II. EXPERIMENT

The chemical structure of the polymer is shown in Fig. 1. Two samples have been synthesized (by Dr. T. Wagner, MPI-P, Mainz) with weight-averaged molecular weights of 1.16×10^4 and 1.5×10^4 g/mol, respectively, and polydispersities of 1.13 and 1.09, respectively (Table I).

PVT measurements were made using a fully automated GNOMIX high-pressure dilatometer. The PVT measurements were made on the PMpTS sample with $M_w = 1.16 \times 10^4$ g/mol. About 1 g was used in the measurements. First, we performed runs by changing pressures from 10 to 200 MPa (1 MPa = 0.01 kbar) in steps of 10 MPa at constant temperatures (i.e., under “isothermal” conditions) from 293 to 403 K. Subsequently, measurements were made by heating/cooling experiments with a rate of 1 K/min at different fixed pressures (i.e., under “isobaric” conditions) in the range from 10 to 200 MPa. The 0.1-MPa data were obtained by extrapolation from the higher pressures. The result from the “isothermal” measurements is shown in Fig. 2 for the different pressures. In the figure it is the relative change of specific volume (ΔV) that is plotted. For the calculation of the thermodynamic parameters such as the thermal expansion coefficient and isothermal compressibility, we have used the literature value for the specific volume of a polydimethylsiloxane with a similar molecular weight ($1.0417 \text{ cm}^3/\text{g}$ at $T = 303 \text{ K}$ and $P = 0.1 \text{ MPa}$).

The setup for the pressure-dependent dielectric measurements consisted of the following parts (described elsewhere in detail): temperature controlled sample cell, hydraulic clos-

TABLE I. VFT and WLF parameters of the two PMpTS samples employed in the present study.

M_w (g/mol)	M_w/M_n	τ_0 (s)	D_T	T_0 (K)	T_g (K)	C_{1T}^g	C_{2T}^g (K)
1.16×10^4	1.3	7×10^{-16}	3.95	203.1	249.9	17.4	45.7
1.5×10^4	1.09	2.5×10^{-14}	2.91	213.9	253.9	14	33.3

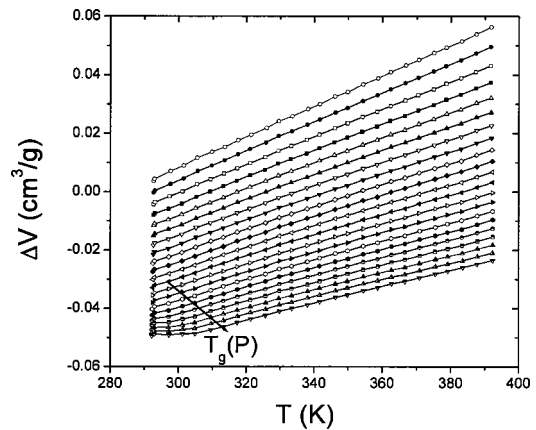


FIG. 2. Relative change in the specific volume (ΔV) of PMpTS ($M_w = 1.16 \times 10^4$ g/mol) as a function of temperature for different pressures in the range from 0.1 to 200 MPa in pressure increments of 10 MPa. The data set at 0.1 MPa is obtained by extrapolation. The lines through the PVT data are guides for the eye. The line indicates the pressure dependence of T_g .

ing press with pump, and pump for hydrostatic test pressure. Silicon oil was used as the pressure-transducing medium. The sample cell consisted of two electrodes with 20 mm in diameter and the sample with a thickness of $50 \mu\text{m}$. The sample capacitor was sealed and placed inside a teflon ring to separate the sample from the silicon oil. The dielectric measurements were made at different temperatures in the range 143–413 K, for pressures in the range from 0.1 to 300 MPa, and for frequencies in the range from 10^{-2} to 10^6 Hz using a Novocontrol BDS system composed from a frequency response analyzer (Solartron Schlumberger FRA 1260) and a broadband dielectric converter. All data were obtained by fixing the temperature (for ten different temperatures: 276.65, 278.75, 280.25, 284.45, 288.15, 290.15, 294.15, 296.15, 300.15, and 304.15 K) and by changing the pressure in steps of 10 MPa, i.e., under “isothermal” conditions. However, the same set of data can also be presented under “isobaric conditions,” i.e., by keeping the pressure fixed and changing temperature. In the latter representation the “isobaric” data obtained at 0.1 MPa over a broader temperature range can be used.

The complex dielectric permittivity $\varepsilon^* = \varepsilon' - i\varepsilon''$, where ε' is the real and ε'' is the imaginary part, is a function of frequency ω , temperature T , and pressure P , $\varepsilon^* = \varepsilon^*(\omega, T, P)$. In Fig. 3, representative dielectric loss spectra are shown under “isobaric” ($P = 0.1 \text{ MPa}$) conditions, and in Fig. 4, spectra are shown under “isothermal” conditions ($T = 278.75 \text{ K}$). A single intense mechanism is shown corresponding to the usual segmental (α) relaxation. However, at lower temperatures another weak relaxation mechanism exists (β process) with a distinctly different T dependence. In the analysis of all DS spectra we have used the empirical equation of Havriliak and Negami (HN) [21],

$$\frac{\varepsilon^*(T, P, \omega) - \varepsilon_\infty(T, P)}{\Delta\varepsilon(T, P)} = \frac{1}{\{1 + [i\omega\tau_{\text{HN}}(T, P)]^\alpha\}^\gamma}, \quad (1)$$

where $\tau_{\text{HN}}(T, P)$ is the characteristic relaxation time in this

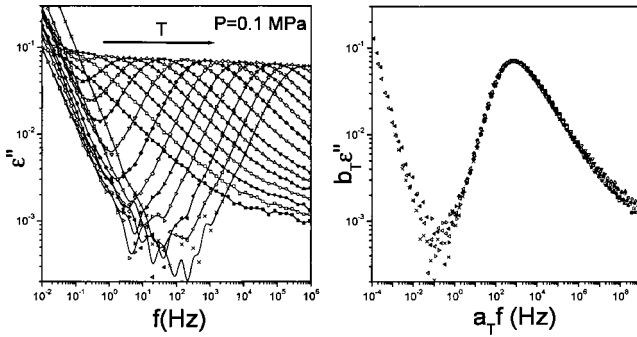


FIG. 3. (Left) Dielectric loss spectra of PMpTS ($M_w = 1.16 \times 10^4$ g/mol) at atmospheric pressure for different temperatures (■, $T = 250.15$ K; □, $T = 252.15$ K; ●, $T = 254.15$ K; ○, $T = 256.15$ K, ▲, $T = 258.15$ K, △, $T = 260.15$ K, ▼, $T = 262.15$ K, ▽, $T = 265.15$ K, ◆, $T = 268.15$ K; ◇, $T = 271.15$ K; ►, $T = 274.15$ K; ▷, $T = 277.15$ K; ◀, $T = 281.15$ K; ◁, $T = 285.15$ K, ×, $T = 289.15$ K). (Right) Same data shifted to the corresponding reference spectrum at $T = 268.15$ K and $P = 0.1$ MPa by applying horizontal (a_T) and vertical (b_T) shifts. Notice that the time-temperature superposition (tTs) holds.

equation, $\Delta\varepsilon(T,P) = \varepsilon_s(T,P) - \varepsilon_\infty(T,P)$ is the relaxation strength of the process under investigation, and α, γ describe, respectively, the symmetrical and asymmetrical broadening of the distribution of relaxation times. In the fitting procedure we have used the ε'' values at every temperature and pressure and in some cases the ε' data were also used as a consistency check. The linear rise of the ε'' at lower frequencies is caused by the conductivity [$\varepsilon'' \sim (\sigma_0/\varepsilon_0)\omega^{-1}$, where σ_0 is the dc conductivity and ε_0 is the permittivity of free space], which has been included in the fitting procedure.

III. RESULTS AND DISCUSSION

The “isobaric” (at 0.1 MPa) and “isothermal” (at 278.75 K) dielectric loss spectra of PMpTS ($M_w = 1.16 \times 10^4$ g/mol) shown in Figs. 3 and 4, respectively, display a single peak originating from the segmental (α -) relaxation process. We attempted to construct master curves by shifting

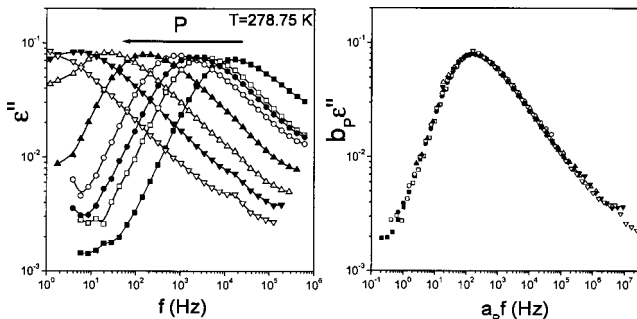


FIG. 4. (Left) Dielectric loss spectra of PMpTS ($M_w = 1.16 \times 10^4$ g/mol) at $T = 278.75$ K for different pressures (■, $P = 0.1$ MPa; □, $P = 7$ MPa; ●, $P = 14$ MPa; ○, $P = 20$ MPa; ▲, $P = 30$ MPa; △, $P = 40$ MPa; ▼, $P = 50$ MPa; ▽, $P = 60$ MPa). (Right) The same data shifted to a reference spectrum at $P = 30$ MPa by applying horizontal (a_P) and vertical (b_P) shifts. Notice that the time-pressure superposition (tPs) holds.

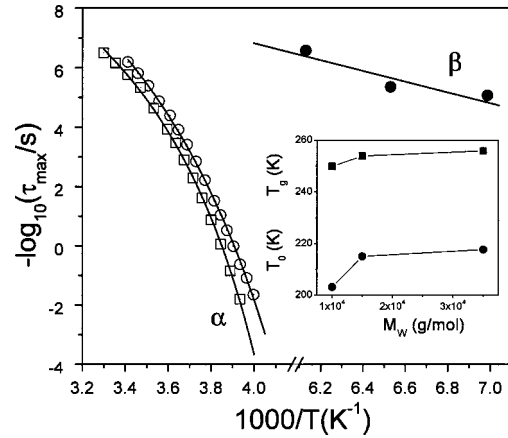


FIG. 5. Arrhenius representation of the relaxation times at maximum loss for the segmental (α) process for two PMpTS: □, $M_w = 1.5 \times 10^4$ and ○, $M_w = 1.16 \times 10^4$ g/mol. The low-temperature relaxation for the $M_w = 1.16 \times 10^4$ g/mol sample is also shown. In the inset we plot the molecular weight dependence of the glass temperature (T_g) (defined as the temperature where the segmental relaxation time is 100 s) and of the “ideal” glass temperature (T_0) for the two samples measured in the present study as well as the one measured in Ref. [14].

each curve of Fig. 3 and Fig. 4 to the α -process maximum loss at a reference T and P , by multiplying the frequency axis of each curve by appropriate shift factors, a_T and a_P , at each T and P . The results of the attempted time-temperature superposition (tTs) and time-pressure superposition (tPs) are shown in the same figures and reveal that tTs and tPs work reasonably well over a broad f - T - P range, meaning that the distribution of relaxation times does not change with temperature or pressure. Small vertical shifts (with factors b_T and b_P) were also required.

As we will see below, there are some intriguing features in the spectra at low T and high P that are not apparent in the superimposed spectra shown. Nevertheless, to a good approximation we can discuss the T and P shift factors. The a_T shift factors can be described by the well-known Williams-Landel-Ferry (WLF) equation

$$\log_{10} a_T = -\frac{c_{1T}^r(T - T_r)}{c_{2T}^r + (T - T_r)}, \quad (2)$$

where c_{1T}^r and c_{2T}^r are the WLF parameters at the reference temperature T_r . The values of the above parameters at T_g for the two PMpTS samples are given in Table I. Similarly, the a_P shift factors can be described by the corresponding WLF equation for the pressure dependence,

$$\log_{10} a_P = \frac{c_{1P}^r(P - P_r)}{c_{2P}^r - (P - P_r)}, \quad (3)$$

where c_{1P}^r and c_{2P}^r are the WLF parameters at the reference pressure P_r . The values of these parameters at a reference pressure of 30 MPa are 13 and 180 MPa, respectively, for the PMpTS sample with $M_w = 1.16 \times 10^4$ g/mol.

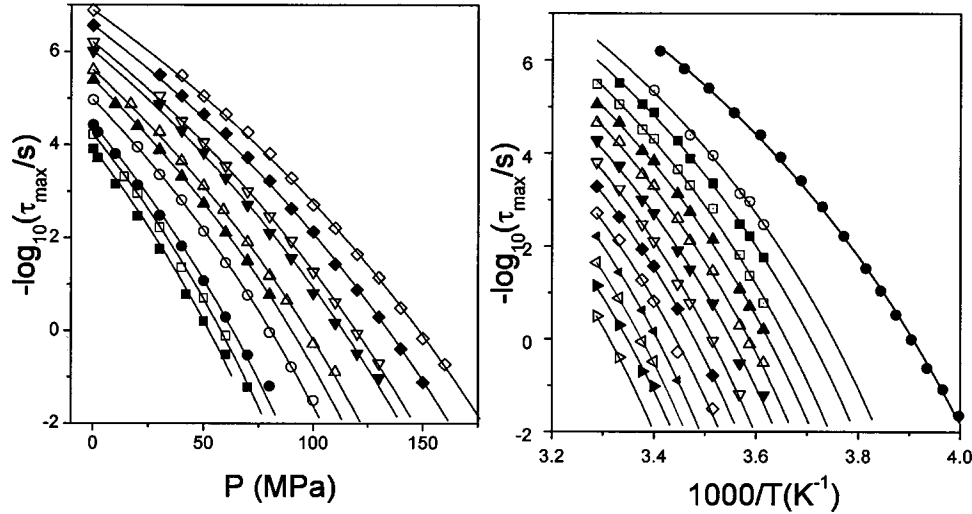


FIG. 6. Pressure (left) and temperature (right) dependence of the relaxation times corresponding to the α -process loss maximum of PMpTS with $M_w = 1.16 \times 10^4$ g/mol. The different symbols are as follows: for the “isothermal” data: \blacksquare , $T = 276.65$ K; \square , $T = 278.75$ K; \bullet , $T = 280.25$ K; \circ , $T = 284.45$ K; \blacktriangle , $T = 288.15$ K; \triangle , $T = 290.15$ K; \blacktriangledown , $T = 294.15$ K; \triangledown , $T = 296.15$ K; \blacklozenge , $T = 300.15$ K; \diamond , $T = 304.15$ K; and for the “isobaric” data: \bullet , $P = 0.1$ MPa; \circ , $P = 20$ MPa; \blacksquare , $P = 30$ MPa; \square , $P = 40$ MPa; \blacktriangle , $P = 50$ MPa; \triangle , $P = 60$ MPa; \blacktriangledown , $P = 70$ MPa; \triangledown , $P = 80$ MPa; \blacklozenge , $P = 90$ MPa; \diamond , $P = 100$ MPa; \blacktriangleleft , $P = 110$ MPa; \triangleleft , $P = 120$ MPa; \blacktriangleright , $P = 130$ MPa; \triangleright , $P = 140$ MPa. The lines represent the result of the fit of the “isothermal” and “isobaric” data to Eqs. (5) and (6), respectively.

The results from the HN fit to the relaxation times at maximum loss for the α as well as for the low-temperature process (β) are depicted in Fig. 5 for the two molecular weights studied here. At low temperatures, the β process displays an Arrhenius T dependence and can be described as

$$\log_{10} \tau_{\max} = \log_{10} \tau_0 + \frac{E}{2.303RT}, \quad (4)$$

where τ_0 is the relaxation time at practically infinite temperature and E ($= 33$ kJ/mol) is the activation energy. The figure conceals the fact that the intensity ($T\Delta\epsilon \sim 0.6$) is very low for this mechanism, suggesting a very localized motion of the side chain bearing the substituted phenyl ring [22]. In contrast, the α process displays a stronger T dependence and can be parametrized according to the Vogel-Fulcher-Tammann (VFT) equation

$$\tau_{\max} = \tau_0 \exp\left(\frac{D_T T_0}{T - T_0}\right), \quad (5)$$

where D_T is a dimensionless parameter and T_0 is the “ideal” glass temperature located below the T_g ($T_0 = T_g - c_{2T}^g$). The VFT parameters for the two different molecular weights investigated here as well as of the one from the literature are summarized in Table I. The molecular weight dependence of T_g and T_0 is plotted in the inset to Fig. 5. Notice that the glass temperature depends on chain length as expected from the higher mobility of the chain ends.

The temperature and pressure dependence of all the relaxation times corresponding to the PMpTS sample with $M_w = 1.16 \times 10^4$ g/mol are summarized in Fig. 6. For the T -dependent relaxation times we have used the VFT equation, whereas for the P -dependent times the pressure equivalent of VFT was employed [23],

$$\tau_{\max} = \tau_{\alpha} \exp\left(\frac{D_P P}{P_0 - P}\right), \quad (6)$$

where τ_{α} is the segmental relaxation time at atmospheric pressure at a given temperature, D_P is a dimensionless parameter, and P_0 is the pressure corresponding to the ideal glass transition. We test the universality of the above equation by plotting the reduced relaxation times as a function of reduced pressure in Fig. 7. The normalized relaxation times fall on a single line with zero intercept and slope $D_P = 42$.

Although the α process seems to obey the tTs and tPs to a good approximation within the limited T and P range shown, the dielectric strength displays some distinct unanticipated features. First, the dielectric strength ($T\Delta\epsilon$) at atmospheric

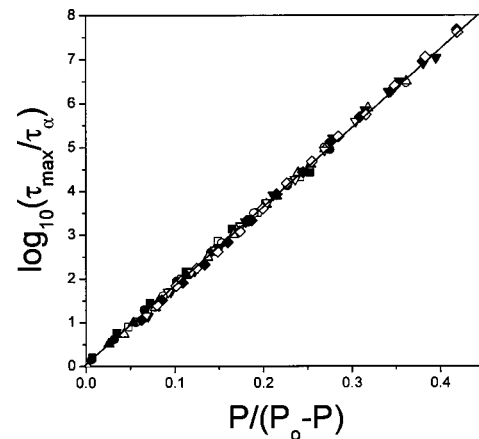


FIG. 7. Pressure dependence of the normalized relaxation times or the α process of PMpTS ($M_w = 1.16 \times 10^4$ g/mol) as a function of reduced pressure for the 10 temperatures shown in Fig. 6. The line is a fit to Eq. (6) with a slope $D_P = 42$.

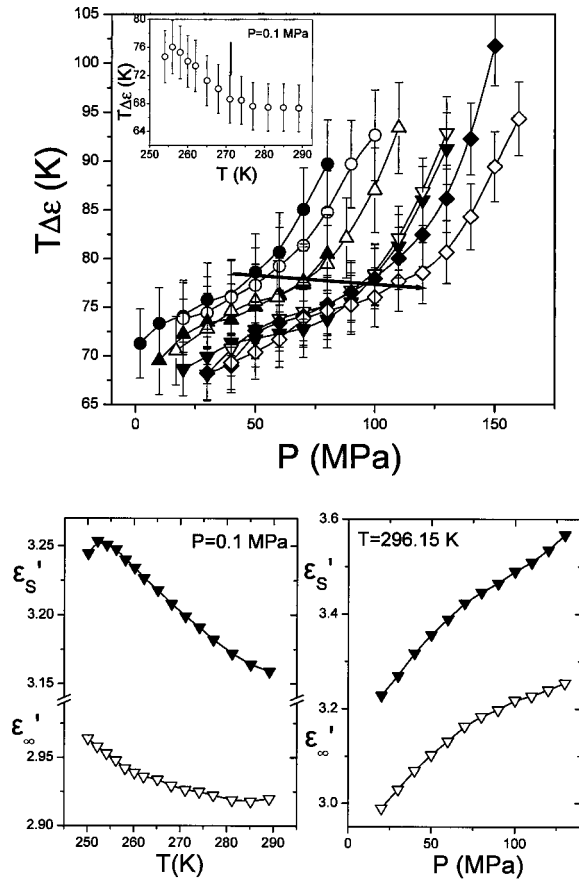


FIG. 8. (a) Pressure dependence of the dielectric strength ($T\Delta\epsilon$) for the α process in PMpTS ($M_w = 1.16 \times 10^4$ g/mol) plotted for different temperatures: \blacksquare , $T = 276.65$ K; \square , $T = 278.75$ K; \bullet , $T = 280.25$ K; \circ , $T = 284.45$ K; \blacktriangle , $T = 288.15$ K; \triangle , $T = 290.15$ K; \blacktriangledown , $T = 294.15$ K; \triangledown , $T = 296.15$ K; \blacklozenge , $T = 300.15$ K; \diamond , $T = 304.15$ K. Notice the strong nonlinear increase of the dielectric strength above a certain critical pressure (shown by the arrow). In the inset the dielectric strength of the same process is plotted as a function of temperature at 0.1 MPa. The vertical arrow indicates that the dielectric strength increases beyond a certain temperature. (b) Relaxed and unrelaxed components of the dielectric constant plotted as a function of temperature (at $P = 0.1$ MPa) and as a function of pressure (at $T = 296.15$ K).

pressure displays an unusual increase below about 270 K (i.e., about 20 K above the glass temperature). This behavior is shown as an inset to Fig. 8(a). The pressure dependence of the relaxation strength shown in Fig. 8(a) for nine temperatures in the range 276.65–301.15 K displays a similar feature; the dielectric strength of the α process first increases with P , reflecting the normal densification, whereas above some critical pressure it strengthens beyond the effect of density. The relaxed (ϵ'_∞) and unrelaxed (ϵ'_S) components of the dielectric constant are shown in Fig. 8(b) as a function of T and P , revealing that the origin of this effect is the higher pressure dependence of the latter component implying the existence of slower relaxations in the spectra as compared to τ_{\max} . It is noteworthy that at the pressures where this sudden increase takes place there is no measurable effect on the dynamics (Fig. 6). The dielectric strength $\Delta\epsilon$ [$=\epsilon'_S - \epsilon'_\infty$,

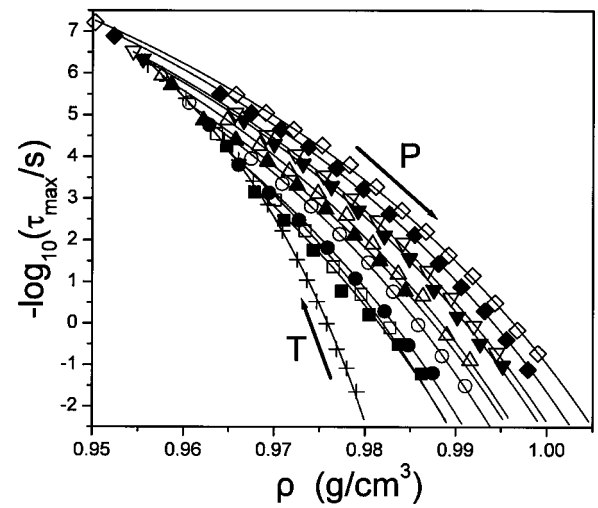


FIG. 9. Arrhenius representation of the relaxation times at maximum loss for the α process of PMpTS ($M_w = 1.16 \times 10^4$ g/mol) as a function of density. The plot combines the “isothermal” times: \blacksquare , $T = 276.65$ K; \square , $T = 278.75$ K; \bullet , $T = 280.25$ K; \circ , $T = 284.45$ K; \blacktriangle , $T = 288.15$ K; \triangle , $T = 290.15$ K; \blacktriangledown , $T = 294.15$ K; \triangledown , $T = 296.15$ K; \blacklozenge , $T = 300.15$ K; \diamond , $T = 304.15$ K obtained by changing pressure at the above isotherms with the “isobaric” times obtained at atmospheric pressure (+) by changing temperature. The arrows indicate the directions of increasing temperature (“isobaric” data) and of increasing pressure (“isothermal” data). The lines are fits to Eq. (8).

where $\epsilon'_S = \lim_{\omega \rightarrow 0} \epsilon'(\omega)$ and $\epsilon'_\infty = \lim_{\omega \rightarrow \infty} \epsilon'(\omega)$] of the segmental mode can be described as

$$\Delta\epsilon \sim \frac{\mu^2}{3k_B T} F g \frac{N}{V}, \quad (7)$$

where μ is the dipole moment for noninteracting dipoles, F ($=[\epsilon_S(\epsilon_\infty + 2)^2/3(2\epsilon_0 + \epsilon_\infty)]$) is the local field correction, g is the Kirkwood-Fröhlich correlation factor giving the angular correlations between the dipoles along the chain, N is the number of dipoles, and V is the volume. The results shown in Fig. 8 suggest a large effect of orientation correlations in PMpTS by decreasing temperature at atmospheric pressure or by increasing pressure at a given temperature. Surprisingly these effects occur in the liquid side of the phase diagram. We recall here that a crossover behavior has been reported for some glass-forming liquids, albeit at a higher frequency range (from 10^7 to 10^8 Hz) [24]. We will return to this point in the discussion of the phase diagram (Fig. 11).

The existence of the PVT data allows casting the T and P dependences of the α -relaxation times in a single representation by using the density as the only variable (Fig. 9). In the figure both “the isobaric” (at $P = 0.1$ MPa) and the “isothermal” sets of data (at the ten different temperatures) are shown. The “isothermal” relaxation times can now be described by a modified VFT equation for the density representation as

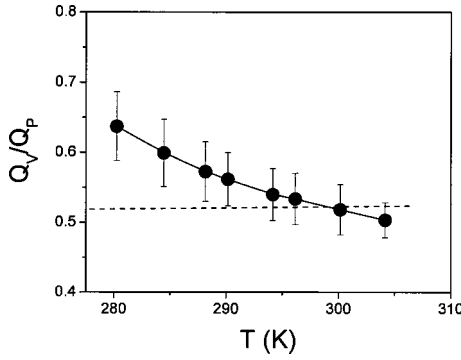


FIG. 10. Temperature dependence of the experimental ratio Q_V/Q_P compared under a density of 0.975 g/cm^3 . In the Q_V and Q_P evaluation the experimental relaxation times of Fig. 6 were used together with the PVT data. The dashed line is the result of the calculation of the same ratio through Eq. (10).

$$\tau_{\max} = \tau_p \exp\left(\frac{D_p \rho}{\rho_0 - \rho}\right), \quad (8)$$

where D_p is a dimensionless parameter and ρ_0 is the density at the ideal glass temperature (T_0). The density representation allows for some conclusions with respect to (i) the validity of free volume theories and (ii) the central parameters controlling glass formation. With respect to (i), the density representation allows access to states with the same density through distinctly different thermodynamic paths obtained by certain T and P variations. Under such conditions, a comparison of the isodensity states reveals distinctly different relaxation times. Under the premise that the fractional free volume and the macroscopic volume have a one-to-one correspondence, this last observation contrasts the predictions of even the simplest free volume theory. With respect to (ii), it is evident from Fig. 9 that in PMpTS, both temperature and density are the important controlling parameters of the segmental dynamics. At a given density, the segmental times are sensitive to the changes in temperature, but at the same time at a given temperature there are strong variations in the relaxation times by changing density (through the pressure variations). Based on this, we conclude that in contrast to some glass-forming liquids and polymers, where temperature appears to be the single control variable of the dynamics, PMpTS segmental dynamics are governed by two parameters, namely density and temperature.

Change in temperature can have two different results: first, purely thermal effects (kT) and second, change in density. In order to decouple the two effects, we need to consider the apparent activation volume at constant density or volume $Q_V(T, V) = -RT^2(\partial \ln \tau / \partial T)_V$ and compare it with the corresponding energy at constant pressure Q_P [$= -RT^2(\partial \ln \tau / \partial T)_P$]. The two energies are related as [25]

$$\left(\frac{\partial \ln \tau}{\partial T}\right)_V = \left(\frac{\partial \ln \tau}{\partial T}\right)_P + \left(\frac{\partial \ln \tau}{\partial P}\right)_T \left(\frac{\partial P}{\partial T}\right)_V, \quad (9)$$

where $(\partial P / \partial T)_V$ is given by the ratio of the thermal expansion coefficient β and the isothermal compressibility κ_T . Then Eq. (9) reduces to

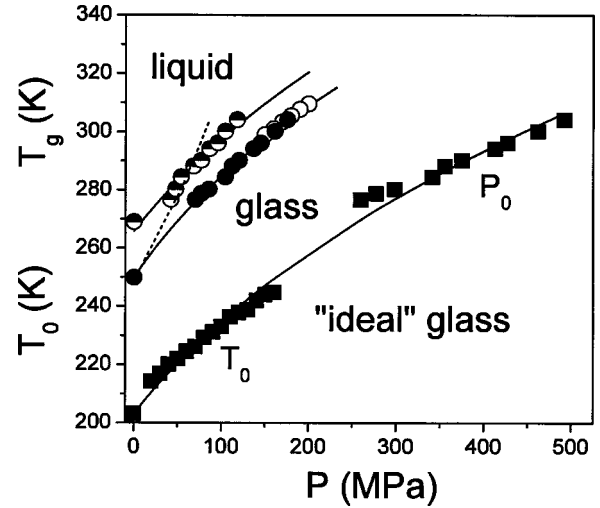


FIG. 11. “Phase diagram” of PMpTS displaying different characteristic regimes: the “ideal” glass, the normal glass, the high-temperature liquid phase, and an intermediate phase possessing higher orientation correlations. The \blacksquare data points reflect the T_0 and P_0 values, the filled circles reflect the $T_g(P)$ (obtained from DS at the temperature where the relaxation times are 100 s), the open circles give the $T_g(P)$ from PVT (at the higher pressures) and the half-filled circles give the critical temperature (at $P=0.1 \text{ MPa}$) and the critical pressures separating two liquids, with and without orientation pair correlations. The dashed line with a slope (dT/dP) = 0.641 K/MPa was calculated at a fixed density (of 0.98 g/cm^3). Notice the stronger dependence of $(dP/dT)_V$ as compared to the $(dP/dT)_{P \rightarrow 0}$.

$$Q_V(T, V) = Q_P(T, P) - \frac{\beta}{\kappa_T} T \Delta V(T, P), \quad (10)$$

where $\Delta V [= RT(\partial \ln \tau / \partial P)_T]$. This quantity is usually called an apparent activation volume. Based on transition state theory, ΔV is interpreted as the difference in the molar volume of activated and nonactivated molecules. Experiments on polyisoprenes [5], however, suggested that at high temperatures (typically $T \sim T_g + 80 \text{ K}$) this volume is comparable to the monomer volume. Consequently, a recent theoretical approach [26] based on the Adam-Gibbs theory of cooperatively rearranging domains suggested a plausible molecular interpretation; ΔV was discussed as the product of the basic molecular unit with the size of the cooperative unit to the second power.

The experimentally obtained ratio Q_V/Q_P is plotted in Fig. 10 as a function of temperature (calculated at a density of 0.975 g/cm^3). This procedure involves plotting the measured relaxation times as a function of T (i) at constant volume and (ii) at constant pressure (for the corresponding pressures obtained from PVT) and the definitions of Q_V and Q_P (some extrapolations were used in the PVT data that result in the error bars shown in the figure). In the same figure the theoretical value of the same ratio is shown calculated from Eq. (10). The results reveal that Q_V/Q_P is in the range from 0.5 to 0.6, suggesting that the rate of the α relaxation reflects largely thermal effects. The same ratio calculated at T_g and at atmospheric pressure amounts to 0.59.

These results can be used to construct a “phase diagram” for PMpTS in Fig. 11. One might question the usefulness of this representation for a liquid, however in view of the results shown here it contains useful information. The construction is based on the pressure dependence of the “ideal” glass temperature $T_0(P)$ and “ideal” glass pressure $P_0(T)$, obtained, respectively, from the “isobaric” and “isothermal” measurements, and of the glass temperature $T_g(P)$ (obtained from the “isobaric” measurements as the temperature where the α -relaxation times are 100 s). The PVT results for the $T_g(P)$ are also included and are in excellent agreement with the dynamically defined $T_g(P)$, revealing that the segmental dynamics follow the thermodynamic state of the system. These dependences can be fitted according to the following empirical equation [12]:

$$T_0(P) = c \left(1 + \frac{b}{a} P \right)^{1/b} \quad (11)$$

with parameters $c = T_0(0) = 203.13$ K, $b = 3.53$, and $\alpha = 5.3$ MPa for the $T_0(P)$ and $P_0(T)$ dependence and $c = 250$ K, $b = 4.58$, and $\alpha = 5.6$ MPa for the $T_g(P)$ dependence. In the figure, we include the data obtained from the pressure dependence of the dielectric strength related to the segmental process, at the critical pressure, i.e., the pressure associated with the onset of strong orientation correlations. The latter dependence can also be described by Eq. (11) using $c = 265.7$ K, $b = 4.5$, and $\alpha = 6.8$ MPa, albeit with a larger uncertainty.

The three solid lines in Fig. 11 separate four regimes. At low temperatures the solid line separates the “ideal” glass from the normal glass phase. At much higher temperatures a pure liquid phase exists, but between the glass and normal liquid another “liquidlike” phase exists with enhanced orientation correlations. The crossover is at approximately $1.08 T_g$ in PMpTS. We recall here that different theoretical approaches predict a transition above the calorimetric T_g . For example, mode coupling theory (MCT) [27] predicts a dynamic transition at a temperature T_c located at approximately $1.2 T_g$ and a two-step segmental relaxation: a “fast” one associated with the segment relaxation within the cage formed by the surrounding molecules and a “slow” one associated with the relaxation of the cage itself. The theory describes polymer and glass-forming liquid dynamics reasonably well at $T \gg T_c$. However, at $T_g < T < T_c$, the idealized MCT fails to account for the dynamics. There are also some reports [28] suggesting a true thermodynamic transi-

tion in polymeric liquids, at a temperature $T_{ll} \sim 1.2 T_g$. The present case reflects a dynamic transition within the liquid phase.

The dashed line in Fig. 11 gives the calculated $T(P)$ dependence under isodensity conditions, with a slope of $(dT/dP)_V \sim 0.64$ K/MPa, which is stronger than the $(dT_g/dP)_{P \rightarrow 0}$ ($= 0.38$ K/MPa) initial slope obtained under conditions of varying density as well. This suggests a simple relation, $(dP/dT_g)_{P \rightarrow 0} = 1.67(dP/dT)_V$ for PMpTS segmental dynamics. Notice that the second part of this equation can be obtained directly from knowledge of the thermodynamic parameters (β and κ_T).

IV. CONCLUSIONS

The investigation of the dynamics in the flexible polymer PMpTS as a function of molecular weight revealed the presence of two channels of relaxation: one below the glass temperature reflecting a localized motion of the substituted phenyl ring with an activation energy of 33 kJ/mol and one above T_g reflecting the segmental dynamics. The main results with respect to the segmental dynamics can be summarized as follows.

(i) In PMpTS there are two control variables of the segmental dynamics: temperature and density. Both have a strong effect on slowing down the α process.

(ii) Distinct thermodynamics (T, P) paths can be chosen resulting in the same density. Under such conditions the segmental relaxation times were found to differ in contrast to any free volume theory. These isodensity states are characterized by an apparent activation energy (Q_V) that is comparable to the corresponding energy under isobaric conditions (Q_P), reflecting the importance of thermal effects.

(iii) There exists a critical pressure signifying the onset of orientation correlations within the liquid side of the phase diagram. This transition is found at temperatures below $1.08 T_g$ and separates a normal liquid at higher temperatures from a correlated liquid at lower temperatures. The analysis of the phase diagram allowed the separation of the influence of the temperature and density on the PMpTS segmental dynamics.

ACKNOWLEDGMENTS

We thank Andreas Best at the Max Planck Institute for Polymer Research, Mainz for the PVT measurements, Dr. Thomas Wagner for the synthesis, and George Tsoumanis for technical support at the University of Ioannina. This work was supported by a GSRT grant (PENED 01ED529).

[1] G. Floudas, in *Broadband Dielectric Spectroscopy*, edited by F. Kremer and A. Schönhal's (Springer, Berlin, 2002), Chap. 8.
 [2] G. Williams, *Trans. Faraday Soc.* **62**, 2091 (1966).
 [3] H. Sasabe and S. Saito, *J. Polym. Sci., Part A-1* **6**, 1401 (1968).
 [4] G. Floudas and T. Reisinger, *J. Chem. Phys.* **111**, 5201 (1999).
 [5] G. Floudas, C. Gravalides, T. Reisinger, and G. Wegner, *J. Chem. Phys.* **111**, 9847 (1999).
 [6] M. Mierzwa, G. Floudas, J. Dorgan, D. Knauss, and J. Wegner,

J. Non-Cryst. Solids **307**, 209 (2002).
 [7] M. Mierzwa, G. Floudas, P. Stepanek, and G. Wegner, *Phys. Rev. B* **62**, 14012 (2000).
 [8] M. Mierzwa and G. Floudas, *IEEE Trans. Dielectr. Electr. Insul.* **8**, 359 (2001).
 [9] G. Floudas, G. Fytas, T. Reisinger, and G. Wegner, *J. Chem. Phys.* **111**, 9129 (1999).
 [10] M. Mierzwa, G. Floudas, M. Neidhoefer, R. Graf, H.W. Spiess, W.H. Meyer, and G. Wegner, *J. Chem. Phys.* **117**, 6289 (2002).

- [11] G. Floudas, M. Mierzwa, and A. Schönals, *Phys. Rev. E* **67**, 031705 (2003).
- [12] S.P. Andersson and O. Andersson, *Macromolecules* **31**, 2999 (1998).
- [13] B.J. PUNCHARD and D. Adolf, *Macromolecules* **35**, 3281 (2002).
- [14] M. Paluch, S. Pawlus, and C.M. Roland, *Macromolecules* **35**, 7338 (2002).
- [15] J.J. Fontanella, C.A. Edmondson, M.C. Wintersgill, Y. Wu, and S.G. Greenbaum, *Macromolecules* **29**, 4944 (1996).
- [16] M. Paluch, K.L. Ngai, and S. Hensel-Bielowka, *J. Chem. Phys.* **114**, 10872 (2001).
- [17] S. Hensel-Bielowka, J. Ziolo, M. Plauch, and C.M. Roland, *J. Chem. Phys.* **117**, 2317 (2002).
- [18] J. Gapinski, M. Paluch, and A. Patkowski, *Phys. Rev. E* **66**, 011501 (2002).
- [19] M.L. Ferrer, C. Lawrence, B.G. Demirjian, D. Kivelson, C. Alba-Simionesco, and G. Tarjus, *J. Chem. Phys.* **109**, 8010 (1998).
- [20] T. Kanaya, A. Patkowski, E.W. Fischer, J. Seils, H. Gläser, and K. Kaji, *Acta Polym.* **45**, 137 (1994).
- [21] S. Havriliak and S. Negami, *Polymer* **8**, 161 (1967).
- [22] N.G. McCrum, B.E. Read, and G. Williams, *Anelastic and Dielectric Effects in Polymeric Solids* (Dover, New York, 1991).
- [23] M. Paluch, A. Patkowski, and E.W. Fischer, *Phys. Rev. Lett.* **85**, 2140 (2000).
- [24] A. Schönals, *Europhys. Lett.* **56**, 815 (2001).
- [25] G. Williams, *Trans. Faraday Soc.* **60**, 1548 (1964); **60**, 1556 (1964).
- [26] C.A. Solunov, *J. Phys. C* **14**, 7297 (2002).
- [27] W. Götze and L. Sjorgen, *Rep. Prog. Phys.* **55**, 241 (1992).
- [28] R.F. Boyer, *Polym. Eng. Sci.* **19**, 732 (1979).